Soft Matter

PAPER

Solvent dependent ordering of poly(3-dodecylthiophene) in thin films†

I. Roy and S. Hazra*

The strong influence of solvents on the ordering of poly(3-dodecylthiophene) (P3DDT) due to edge-on oriented stacking, in the spin-coated thin film on the Si substrate, both near the substrate and away from it, depending upon the substrate surface nature, is observed from the X-ray reflectivity study. The absence of any appreciable amount of coil-like P3DDT chains (*i.e.* charge localized states) and formation of π-stacked aggregates (*i.e.* charge delocalized states) in the spin-coated thin films, with slightly better uniformity for the film prepared from toluene (TL) compared to that prepared from chloroform (CF) and chlorobenzene (CB), are well evident from the optical absorption study. No ordering near the weakly hydrophobic H–Si substrate is found in the films prepared from TL, probably due to less diffusion of P3DDT in TL and the appreciable pinning (film–substrate interaction) effect, while appreciable ordering near the film–air interface, overcoming the pinning effect, is likely to be related to the moderate values of the viscosity and the evaporation rate of the solvent. A better ordered Form-I-like relaxed structure near the film–substrate interface and a less ordered interpenetrating Form-II-like structure toward the film–air interface are found in the films prepared from CF, probably related to the low viscosity and high evaporation rate, respectively, of the solvent. Less ordered and mixed but more toward Form-II-like structures are formed throughout the film prepared from CB, probably due to the high viscosity of the solvent, even though its evaporation rate is low. The high evaporation rate of CF and high viscosity of CB probably create hindrance in the formation of continuous films on the weakly hydrophilic O–Si substrate at low speed, while the moderate values of both the parameters for TL, help to form continuous films on the O–Si substrate even at low speed. Such moderate values also help to form less variable (and more toward Form-I-like) structures and better ordering in the latter film. The relative fluctuation between aggregates along the film-thickness is, however, found slightly more in the film prepared from TL compared to that prepared from CF.

1 Introduction

Semiconducting organic molecules and polymers are becoming increasingly important in the electronics industry due to their flexibility, easier fabrication and low cost. Ordering and orientation of such molecules significantly influence the physical properties of organic materials and their corresponding device properties. Therefore ordering organic molecules, especially conjugated polymer molecules, in the active layer has been a hot topic in organic electronics due to their high performance.[1–5] Poly(3-alkylthiophenes) (P3ATs) are one such kind of polymer having flexible alkyl side chains attached to stiff backbones consisting of thiophene units. They are soluble in a variety of common organic solvents which makes it possible for the fabrication of devices using simple solution processing techniques.[6] They are semi-crystalline in nature,

having crystalline P3AT domains as well as amorphous regions. The chemical incompatibility between the alkyl side chains and the polythiophene backbone is responsible for the crystalline ordering of the polymer.[7–9] P3AT molecules can adopt two types of orientation on a substrate-(i) edge-on orientation, in which lamellae are perpendicular to the substrate, and (ii) face-on, in which they are parallel to it.[6]

The field-effect mobility of devices strongly depends on the orientation and ordering of the P3AT molecules which in turn depend on various factors such as regioregularity and molecular weight,[10] the length of the alkyl side chain,[11] the solvent from which the film is cast,[12] the nature of the substrate[13–15] and deposition techniques like drop-casting, spin-coating, dip-coating and directional epitaxial crystallization.[16,17] It has been pointed out that the mobility in films having *edge-on* orientated molecules and *face-on* oriented molecules differ by more than a factor of 100.[6] Mobility increases with increasing molecular weight of the polymer as longer chains provide longer paths for the charge carriers to travel without hopping to another chain.[10] When several polymer chains are locally aligned they have a strong wave

*Saha Institute of Nuclear Physics, 1/AF Bidhannagar, Kolkata 700064, India.
E-mail: satyajit.hazra@saha.ac.in*

function overlap which leads to π-stacking. This π-stacking causes the charge carriers and excitons in P3AT to delocalize along the conjugated polymer backbones over several neighboring chains.[18,19] Improving the π-stacking is thus an important issue in preparing efficient devices using P3ATs. Post-deposition treatments such as annealing have also been reported to influence the orientation of the crystalline domains.[20] Another factor that affects the stability of these films is the ambient atmosphere. P3AT films are extremely stable under humidity and atmospheric oxygen but are affected to a much greater extent by volatile organic solvents.[21,22] So, the understanding of the various processes that control the morphology of these films is crucial for the sake of fabricating devices with high charge carrier mobility and in this direction the continuous effort is on going.

P3AT with longer alkyl side chains, such as poly(3-dodecyl-thiophene) (P3DDT), is found to give rise to stronger photo-luminescence[23] and electroluminescence[24] intensities than P3ATs with shorter alkyl chains. Even then, P3DDT is less studied due to its low crystallizability arising from longer side chain inter-actions.[9,25–30] However, longer alkyl chains of P3DDT are responsible for their better solubility, which helps to make better continuous and relatively smooth films, useful for device applications. The understanding of ordering in such films and its correlation with different process parameters is absolutely necessary to select the appropriate process parameters for this material for its particular use and even for its further enhance-ment of ordering. It is known that the surface free energy or the varying potential energy landscape of the substrate surface can control the substrate–polymer interactions and thus the orientation, ordering and packing of the molecules near the interface.[13,14] Similarly, the solvent can also influence the substrate–polymer interactions and thus the interfacial and subsequent structures of the film. However, not much work has been carried out to understand such influence, which is very important. The thick-ness of a thin film and its ordering or layering can be well estimated using a X-ray reflectivity (XR) technique.[31–37] The XR technique essentially provides an electron-density profile (EDP), *i.e.*, in-plane (*x*–*y*) average electron density (ρ) as a function of depth (*z*) in high resolution. From the EDP it is possible to estimate the total film thickness (*D*), roughness (σ) and ordering or bilayer separation (*d*) of alternate layers of polythiophene backbones and alkyl chains, if any. It also provides unique structural information about the film near the film–substrate interface, which not only influences the subsequent structure of the film but also the device properties or performances.[13,15]

In this paper we have utilized this XR technique to investi-gate the effect of concentration of the polymer, solvent, sub-strate surface nature and spinning speed on the out-of-plane structure or the morphology of the spin-coated P3DDT thin films on silicon, with special emphasis on the structure near the film–substrate interface. Formation of π-stacked aggregates in the spin-coated P3DDT thin films is confirmed from the optical absorption spectra. The strong influence of solvents has been observed in the ordering of the films. The possible parameters of the solvent, which may influence such ordering in the films, both near the substrate and away from it, are discussed.

2 Experimental

Regioregular P3DDT was purchased from Sigma-Aldrich (average molecular weight: 60 000, regioregularity ≥98.5%) and used as received. Chloroform (CF, CHCl₃) and toluene (TL, C₇H₈) were obtained from Merck and chlorobenzene (CB, C₆H₅Cl) was obtained from Sigma-Aldrich. Polymer solutions were prepared by dissolving different amounts of P3DDT in CF, CB and TL solvents. The concentration of the polymer in CF and CB solutions varies from 1 to 4 mg ml^{-1}, while that in TL solution varies from 1 to 3 mg ml^{-1}. H-terminated Si (H–Si) substrates were prepared through the standard pre-treatment method.[38–42] In short, Si substrates (of size about 15 × 15 mm²) were first sonicated in acetone and ethanol solutions to remove organic contaminants and subsequently etched with hydrogen fluoride [HF, Merck, 10%] solution for 60 s at room temperature (25 °C) to terminate the Si surface with H after removing the native oxide layer. Films were then prepared from different polymer solutions on the H–Si substrates using a spin-coater (SCS 6800 Spin Coater Series) at a speed of 3500 rpm for 60 s and were labeled as *c*-SV, where *c* represents the concentration of the polymer and SV represents the solvent (*i.e.* CF, TL or CB). To check the effect of the substrate surface nature on the film structure, films were also prepared from some of the solutions on the clean native oxide coated Si (O–Si) substrates at the same speed (3500 rpm). For the optical study films of nearly similar thickness were prepared on the clean quartz glass substrates at the same speed (3500 rpm). A set of films was prepared from a P3DDT–TL solution on O–Si substrates by changing the spinning speed (ω) from 500 to 4000 rpm. However, continuous films could not be prepared from P3DDT–CF and P3DDT–CB solutions on O–Si substrates for low (≤1000 rpm) spinning speed.

XR measurements of the films were performed on a versatile X-ray diffractometer (VXRD) setup.[9,40,42,43] VXRD consists of a diffractometer (D8 Discover, Bruker AXS) with a Cu source (sealed tube) followed by a Göbel mirror to select and enhance Cu Kα radiation (λ = 1.54 Å). The diffractometer has a two-circle goniometer [θ(ω) − 2θ] with a quarter-circle Eulerian cradle as the sample stage. The latter has two circular (χ and ϕ) and three translational (X, Y, and Z) motions. The scattered beam was detected using a NaI scintillation (point) detector. Data were taken under the specular condition, *i.e.*, the incident angle, α, is equal to the reflected angle, β ($\alpha = \beta = \theta$). Under such conditions there exists a nonvanishing wave vector component, q_z, which is equal to $(4\pi/\lambda)\sin\theta$ with a resolution of 0.002 Å^{-1}.

Optical absorption spectra of the spin-coated P3DDT films of similar thickness deposited from different solvent solutions on quartz substrates were collected using a UV-vis spectro-photometer (Perkin Elmer, Lambda 750).[9]

3 Results and discussion

3.1 X-ray reflectivity and electron-density profiles

XR data of the spin-coated P3DDT thin films on H–Si substrates for different concentrations of the polymer dissolved in CF, TL and CB solvents are shown in Fig. 1–3, respectively. Oscillations or Kiessig

fringes, which are the measure of the total film thickness, are very clearly evident in all the XR profiles. A broad hump (around $q_z \approx 0.24$ Å^{-1}) or modulation in the Kiessig fringes with prominent fall in the fringes' intensity after $q_z \approx 0.26$ Å^{-1} is also observed in all the XR profiles. Such modulation provides the existence of some layering or ordering in the system. The value of d-spacing obtained from the position of the hump is about 2.6 nm, which is suggestive of an edge-on orientation of the polymer chains. The number of Kiessig fringes, hence the film-thickness, increases with concentration, as expected. The Kiessig fringes and the modulation also depend on the solvent, apart from the concentration, which are clearly evident in Fig. 4 and 5, where the XR profiles of films prepared from three different solvents are plotted for comparison. The number of fringes is minimum for the films prepared from CB solvent, while maximum for the films prepared from CF solvent (see Fig. 4). That means more polymer is required for TL solvent compared to CF solvent and even more for CB solvent to get similar number of fringes (see Fig. 5). On the other hand, the amplitude of modulation is minimum for the films prepared from TL solvent, while nearly the same for the films prepared from CF and CB solvents.

To get the quantitative information about the films, all XR profiles have been analyzed using Parratt's formalism[44] after incorporating roughness at each interface. It is necessary to mention that a single layer above the substrate cannot fit the data. Similarly, two layers above the substrate, one for the interfacial layer and another for the remaining portion, can create some modulation but cannot fit the data completely
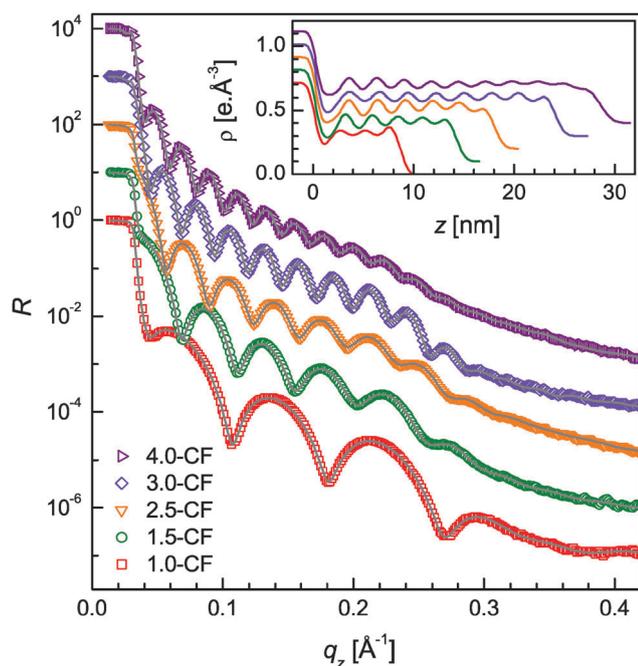

Fig. 2 XR data (different symbols) and analyzed curves (solid lines) of the spin-coated P3DDT thin films deposited from solutions of different concentrations of the polymer in the toluene (TL) solvent. Inset: the corresponding analyzed EDPs. Curves and profiles are shifted vertically for clarity.

Fig. 1 XR data (different symbols) and analyzed curves (solid lines) of the spin-coated P3DDT thin films deposited from solutions of different concentrations of the polymer in the chloroform (CF) solvent. Inset: the corresponding analyzed EDPs. Curves and profiles are shifted vertically for clarity.
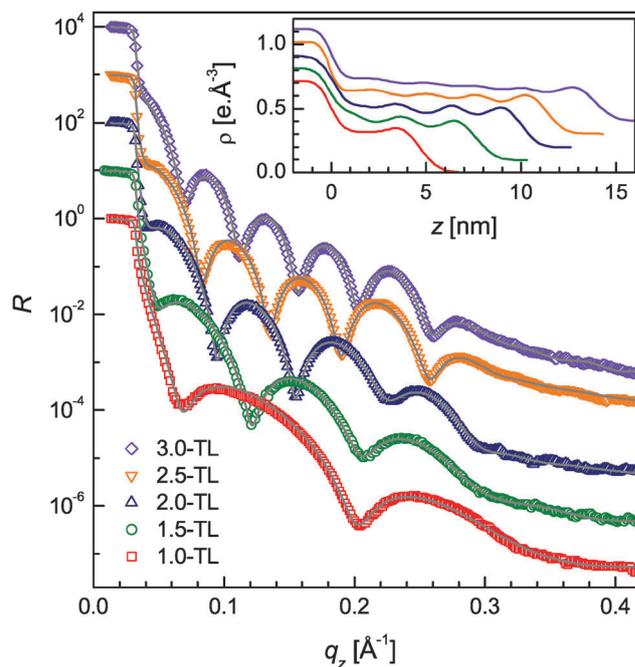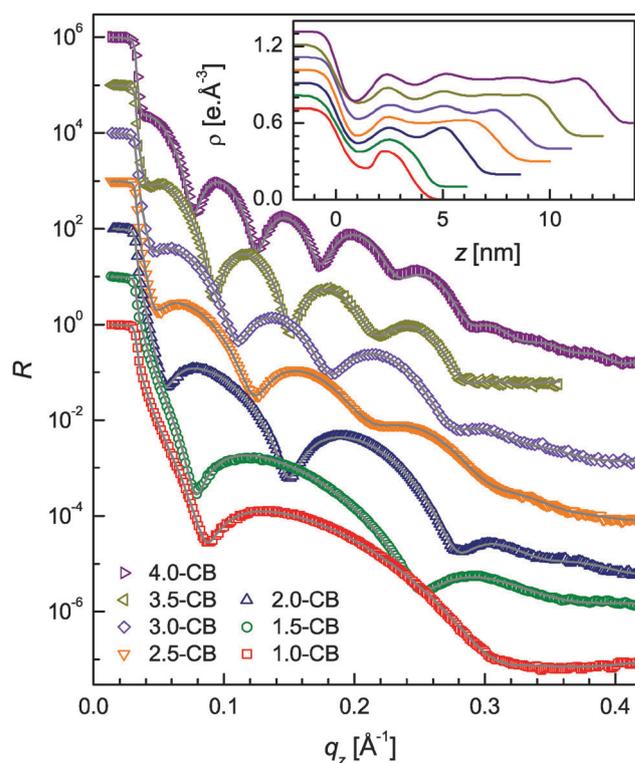

Fig. 3 XR data (different symbols) and analyzed curves (solid lines) of the spin-coated P3DDT thin films deposited from solutions of different concentrations of the polymer in the chlorobenzene (CB) solvent. Inset: the corresponding analyzed EDPs. Curves and profiles are shifted vertically for clarity.
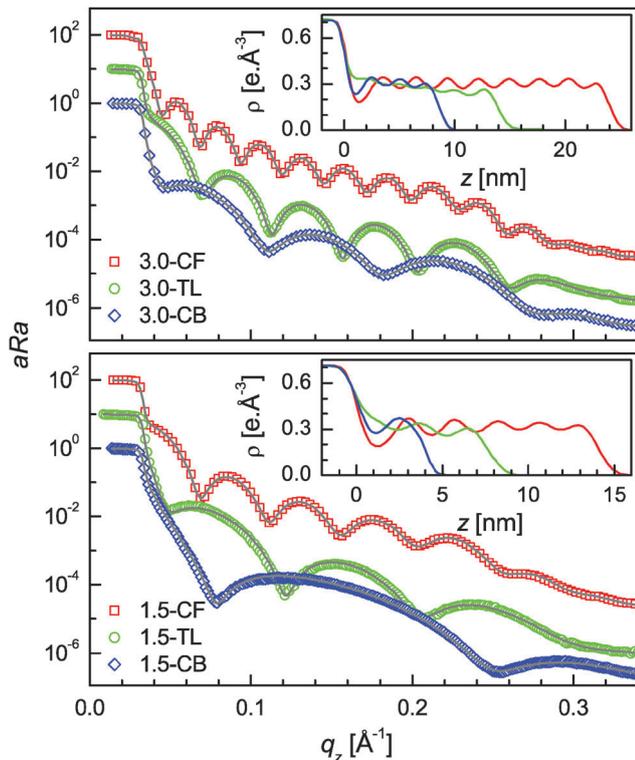
Fig. 4 XR data (different symbols) and analyzed curves (solid lines) of the spin-coated P3DDT thin films deposited from solutions of two concentrations (3.0 and 1.5 mg ml^{-1}) of the polymer in different solvents (curves are shifted vertically for clarity). Insets: the corresponding analyzed EDPs.
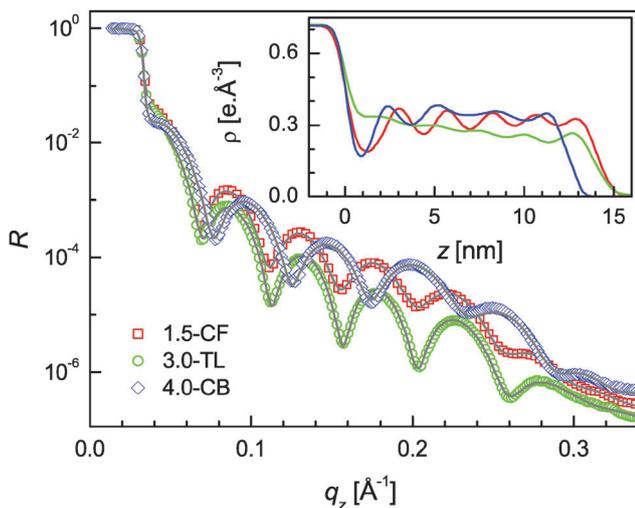

Fig. 5 XR data (different symbols) and analyzed curves (solid lines) of the spin-coated P3DDT thin films of nearly the same thickness deposited from solutions containing different concentrations of the polymer in different solvents. Inset: the corresponding analyzed EDPs.

(as shown in Fig. S1–S3 of the ESI†). Especially it cannot reproduce the sudden decrease in the intensity of Kiessig fringes after $q_z \approx 0.26$ Å^{-1}. Thus for the analysis, each film has been divided into a number of bilayers after the interfacial layer. Each bilayer of thickness about 2.6 nm is constituted of

two parts: alkyl side chains (low electron density) and polythiophene backbones (high electron density). The best fit XR profiles along with the corresponding EDPs are shown in Fig. 1–5. The ordering in the film above the interfacial region is found to vary with the solvent and concentration. Also the EDPs for the films prepared from TL solvent show a broad hump, while for the films prepared from CF and CB solvents show a dip near the film–substrate interface. This indicates that the attachment and orientation of the polymer with the substrates for the TL solvent is different from that for the CF and CB solvents.

In order to understand the effect of the substrate nature on the structure of the film, XR data of P3DDT thin films on H–Si and O–Si substrates for the polymer dissolved in CF, TL and CB solvents are shown in Fig. 6. There is almost no substrate effect in the XR profiles for the films prepared using CF and CB solvents, while in the XR profiles for the films prepared using TL solvent, the hump near $q_z \approx 0.24$ Å^{-1} is found prominent for the film on the O–Si substrate compared to that on the H–Si substrate. To get the quantitative information about the films, all XR data are analyzed as before and the best fit XR profiles
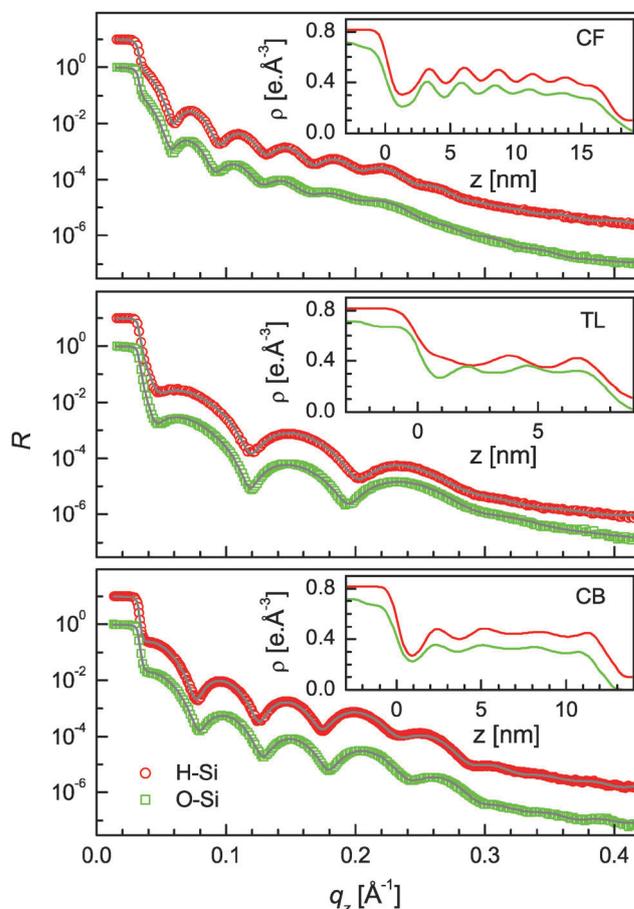

Fig. 6 XR data (different symbols) and analyzed curves (solid line) of the spin-coated P3DDT thin films on H–Si and O–Si substrates deposited from solutions containing the polymer in different solvents. Inset: the corresponding analyzed EDPs. Curves and profiles are shifted vertically for clarity.

along with the corresponding EDPs are shown in Fig. 6. It is clear from the EDPs that the structures of the films on H–Si and O–Si substrates are almost the same for the films prepared from either CF or CB solvent, while different for the films prepared from TL solvents. For the latter a broad hump near the film–substrate interface is observed on the H–Si substrate (as observed before and shown in Fig. 2), while a dip near the film–substrate interface is observed on the O–Si substrate. This indicates that the attachment and orientation of the polymer on the O–Si substrate prepared using TL solvent is similar to that prepared using CF or CB solvents on either H–Si or O–Si substrate.

The XR data of the P3DDT thin films on O–Si substrates prepared from a P3DDT–TL solution at different spinning speeds are shown in Fig. 7. The XR data of the limited number of films that could be prepared from P3DDT–CF and P3DDT–CB solutions on the O–Si substrates due to the speed variation are not included here. The number of Kiessig fringes, hence the film-thickness, in the XR curves, decreases with the increase of the spinning speed, as expected. A broad hump near $q_z \approx$ 0.24 Å^{-1} is also observed for all the films, which is particularly prominent for the high thickness (slow speed) films. To get the quantitative information about the films, all XR data are again analyzed as before and the best fit XR profiles along
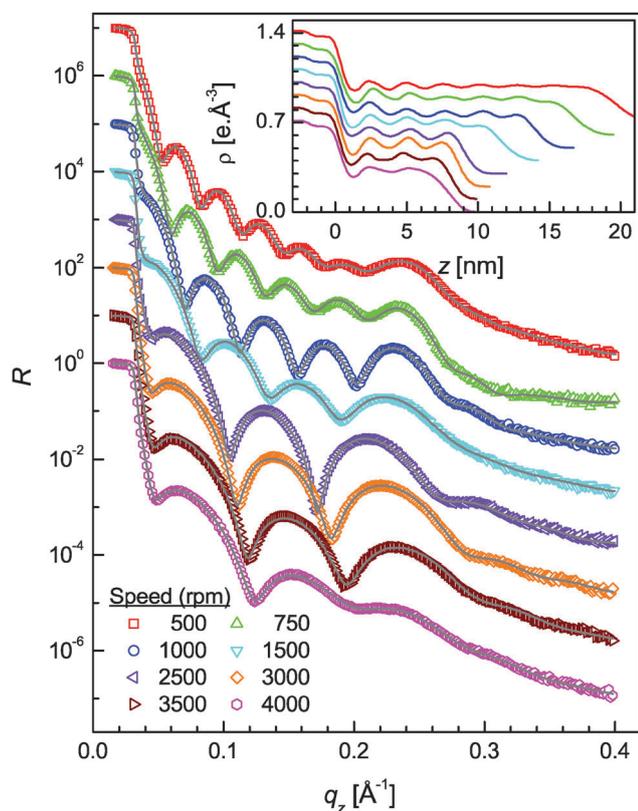
with the corresponding EDPs are shown in Fig. 7. A dip near the film–substrate interface is found for all the films. The ordering is also obvious in the film, which varies with the film-thickness.

3.2 Optical absorption and π-stacking

The UV-vis absorption spectra of three spin-coated P3DDT thin films of similar thickness on quartz glass substrates prepared using CF, TL and CB solvents are shown in Fig. 8. Considering the information of Fig. 5, 1.5-CF, 3.0-TL and 4.0-CB solutions were used to get similar film-thickness from different solvents. Four shoulders/peaks are visible in all the spectra. The peaks near 490 and 610 nm are well resolved, while the peaks near 530 and 560 nm are not, especially for the 1.5-CF and 4.0-CB films. The appearance of peaks may originate from π-stacking of P3AT.[9] The peak at 610 nm is due to the interchain π–π transition, while the peaks at 560, 530 and 490 nm are due to the 0–0, 0–1 and 0–2 transitions of the intrachain exciton.[45] The observed spectral signatures can be interpreted considering the weakly interacting HJ-aggregate model, where the intensity ratio (A_1/A_2) of the peaks at 610 and 560 nm can be used to extract the free exciton bandwidth of the aggregates (based on Frank-Condon analysis), which is related to the coupling strength and the conjugation length.[46,47] Thus considering both the interpretations, the presence of aggregates or lamellae structures due to π-stacking is clearly evident in all the spin-coated films. Also, a similar value of A_1/A_2 (about 0.6) for all the films suggests that the coupling strength or the conjugation length for different films is comparable. The absence of a peak near 450 nm (which appears due to coil-like P3DDT chains comprising twisting and bending of the thiophene rings) indicates the absence of any appreciable amount of coil-like P3DDT chains in the films. The peak at 490 nm can also appear from the intrachain π–π transition of the planar rod-like

Fig. 7 XR data (different symbols) and analyzed curves (solid lines) of the spin-coated P3DDT thin films deposited on O–Si substrates at different spinning speeds from a solution of polymer dissolved in TL solvent. Inset: the corresponding analyzed EDPs. Curves and profiles are shifted vertically for clarity.
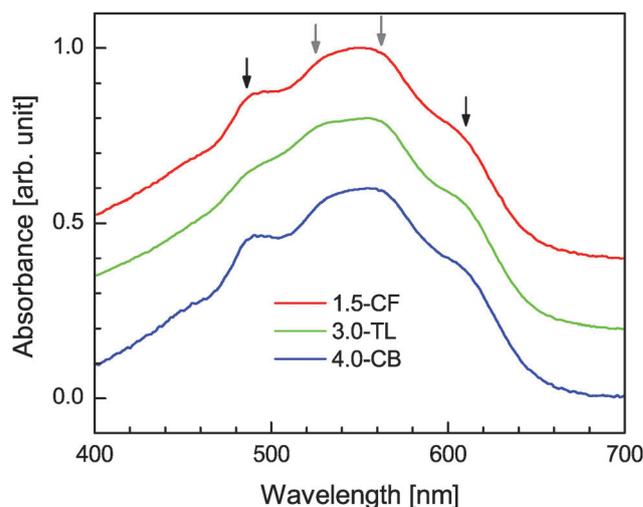

Fig. 8 UV-vis spectra of the spin-coated P3DDT thin films of similar thickness on glass substrates prepared using CF, TL and CB solvents. Peak positions are indicated by arrows.

conformation of the P3DDT chains. Thus the slightly intense peak at 490 nm for the 1.5-CF and 4.0-CB films compared to the 3.0-TL film indicates the presence of comparatively more free rod-like chains in the former two. The less intense 490 nm peak and better resolved 530 and 560 nm (A_3 and A_2) peaks for the 3.0-TL film compared to the others indicate that the structure of the former one is slightly different. This in general suggests that the structures of the films prepared using TL solvent are slightly different from those prepared using CF and CB solvents. In particular, the structures of the aggregates in the films on glass substrates seem to be more uniform or similar for the film prepared using TL solvent compared to those prepared using CF and CB solvents, as less uniform or dissimilar structures of aggregates will place A_2 and A_3 bands in slightly varying positions to show a smearing effect, while similar structures of aggregates will place those bands in more unique positions and will be better resolved.

3.3 Structures of spin-coated P3DDT thin films

Let us now try to understand the ordering of the polymer, which forms the basis of the structures of the film, in greater detail. The ordering of the polymer in a film can be understood considering the variation of the bilayer thickness in it and the density contrast between two parts of a bilayer. A small variation and large contrast indicate better ordering, while a large variation and small contrast indicate the reverse. Thus information on both the parameters is important. In addition the information about the attachment of the film with the substrate is also important. In this view, the thickness (d) and the electron density contrast ($\Delta\rho$) for different bilayers starting from the substrate for all the films are plotted in Fig. 9. The value of $\Delta\rho$ for $N = 0$ indicates the electron density difference between the substrate and the film at the film–substrate interface. The value of this $\Delta\rho$ for the films deposited from CF and CB solvents is greater than 0.4 e Å^{-3}, while that for the films deposited from TL solvent on H–Si substrates is less than 0.4 e Å^{-3} but on O–Si substrates is again greater than 0.4 e Å^{-3}. It can be noted that the difference between the substrate electron density and the average film electron density is about 0.4 e Å^{-3}. The electron density deviation ($\Delta\rho_{in}$) near the interface from the average film electron density (ρ_a) for the four sets of films is tabulated in Table 1. The positive and negative signs indicate humps and dips, respectively. The value of the interfacial thickness (d_{in}), i.e. the value of d for $N = 0$, which represents the width of the first hump or dip is indicated in Table 1. The dip followed by a peak indicates that the attachment of the film with the substrate is through alkyl side chains of the predominantly edge-on oriented polymer. The absence of a dip indicates no preferential attachment
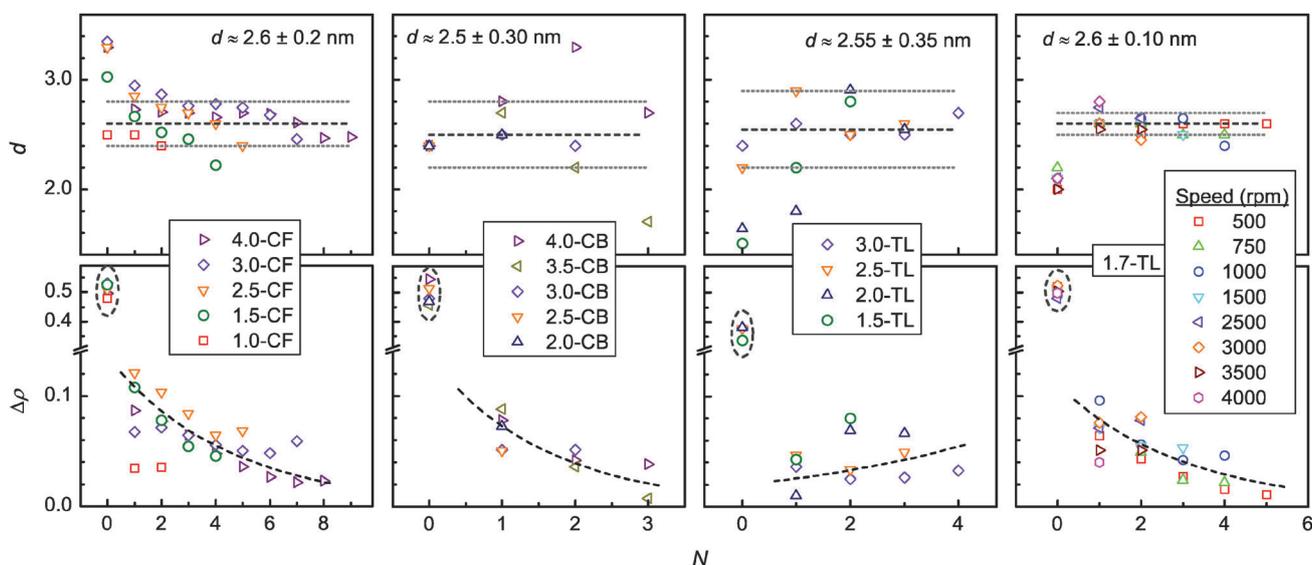

Fig. 9 Variation of the bilayer thickness (d) and the bilayer electron density contrast ($\Delta\rho$) with a number of layers (N) for different spin-coated P3DDT thin films.

Table 1 Parameters, such as the average electron density (ρ_a) of the film, its deviation ($\Delta\rho_{in}$) near the film–substrate interface to form a dip/hump ($-$/$+$) of certain thickness (d_{in}), the average bilayer thickness (d) with its standard deviation (σ_d), the maximum electron density contrast ($\Delta\rho_m$) and the exponential decay length (ξ) for the P3DDT thin films prepared from solutions containing either chloroform (CF), chlorobenzene (CB) or toluene (TL) solvents on H–Si or O–Si substrates by varying the polymer concentration (c) or the spinning speed (ω)

Solvent	Substrate	Variation	ρ_a (e Å^{-3})	$\Delta\rho_{in}$ (e Å^{-3})	d_{in} (nm)	$d_a \pm \sigma_d$ (nm)	$\Delta\rho_m$ (e Å^{-3})	ξ (nm)
CF	H–Si	c	0.30 ± 0.02	-0.08 ± 0.03	3.0 ± 0.4	2.60 ± 0.20	0.14	11.4
CB	H–Si	c	0.30 ± 0.02	-0.08 ± 0.05	2.4 ± 0.1	2.50 ± 0.30	0.14	4.0
TL	H–Si	c	0.30 ± 0.02	$+0.04 \pm 0.02$	2.0 ± 0.5	2.55 ± 0.35	0.02	-10.0
TL	O–Si	ω	0.30 ± 0.02	-0.08 ± 0.02	2.1 ± 0.1	2.60 ± 0.10	0.11	7.8

and/or orientation of the polymer. The value of the width of the dip is found to vary, which is the maximum for the films prepared using CF solvent and minimum for the films on the O–Si substrates prepared using TL solvent.

For the films where a dip is present at the film–substrate interface, the value of $\Delta\rho$ after the interfacial region is found to be maximum, which decreases gradually toward the top surface. The situation is however reverse for the film where the hump is present at the interface. Such a variation in $\Delta\rho$ can be expressed using the standard exponential decay function:

$$\Delta\rho(N) = \Delta\rho_m \exp(-Nd_a/\xi)$$

where $\Delta\rho_m$ is the maximum value of $\Delta\rho$, d_a is the average d value and ξ is the critical decay length. The values of these parameters are tabulated in Table 1. The negative value of ξ essentially indicates exponentially increasing nature of $\Delta\rho$, where $\Delta\rho_m$ is the minimum value. The value of d is found to vary with film-thickness. The standard deviation (σ_d) of which is included in Table 1 along with the value of d_a. In general, the electron density profile of the film from the first peak (after a dip or hump near the interface) can be expressed as:

$$\rho(z) = \rho_a + \frac{1}{2}\Delta\rho_m e^{-z/\xi} \cos\left(\frac{2\pi z}{d_a \pm \sigma_d}\right)$$

The small $\Delta\rho_m$-value, the large negative ξ-value and the large σ_d-value for the films prepared using TL on the H–Si substrate are indicative of the poor ordering in the film due to the absence of the preferential attachment and/or orientation of the polymer near the substrate. The value of $\Delta\rho_m$ for the films prepared using CF and CB solvents are relatively high. Among them the value of ξ and σ_d for the films prepared using CF solvent are comparatively large and small, respectively, suggesting that the ordering in this film is better. On the other hand, although the value of $\Delta\rho_m$ and ξ for the films prepared using TL solvent on the O–Si substrates are small compared to those for the films prepared using CF solvent, the small value of σ_d for the former provides quite good ordering.

The structure of the film can be better understood combining the information on ordering from EDP with aggregates from optical absorption, which are schematically shown in Fig. 10. The attachment and the orientation of the polymer with the substrate strongly depend on the solvent and/or with the nature of the substrate. Such differences is generally related to diffusion, adsorption and pinning effects.[48] The substrate surface nature can be modified through termination of the surface with different groups, which essentially modifies the surface free energy, polar–nonpolar (hydrophilic–hydrophobic) or electrostatic nature of the surface.[34,38–42] It is clear that such surface free energy or the potential energy landscape of the substrate surface, which is generally known to control the substrate–polymer interactions,[13,14] is necessarily modified differently depending upon the solvent environment. The different properties of the solvents, which can give rise to the different polymer–solvent interactions, are tabulated in Table 2. Our results suggest that the diffusion of polymers in the TL solvent is less (may be due to low mass density and dipolarity values[49,50])
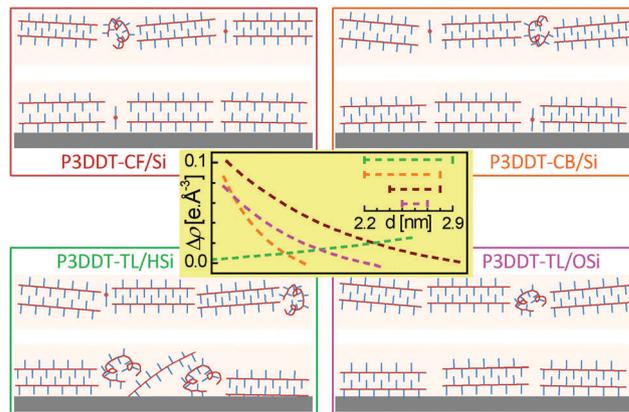

Fig. 10 Variations of $\Delta\rho$ and d, to represent the ordering of P3DDT, in four systems. The corresponding schematic illustration of the structures of the spin-coated P3DDT films on H–Si and O–Si substrates prepared using chloroform (CF), chlorobenzene (CB) and toluene (TL) solvents, showing the effect of the substrate nature and the solvent on the attachment, orientation and ordering of P3DDT near film–substrates and film–air interfaces.

Table 2 The mass density (ρ_m), the viscosity (η_0), the evaporation rate (E) and the dipolarity (SdP) for different solvents, as obtained from literatures or online sites[49–52]

Solvent	ρ_m (g ml^{-1})	η_0 (cP)	E	SdP
Chloroform	1.48	0.54	11.6	0.614
Toluene	0.87	0.55	2.4	0.284
Chlorobenzene	1.11	0.75	1.1	0.537

compared to those in the CF and CB solvents, at least near the substrate, while the tendency of adsorption on the H–Si substrate seems to be slightly more compared to that on the O–Si substrate (due to the difference in the hydrophobic/hydrophilic nature). The effect of adsorption is only noticeable when the diffusion is small, accordingly there is pinning and less ordering on the H–Si substrate, while less pinning and better ordering on the O–Si substrate for the polymer containing TL solvent. On the other hand, when the diffusion is relatively large then the pinning is less and the ordering is better on the substrate, independent of its nature (H–Si or O–Si), as observed for the films prepared using CF and CB solvents. The d-value in the polymer aggregates prepared using CF and CB solvents has large variation (i.e. less uniform) compared to that prepared using TL solvent on the O–Si substrate. However, the variation is systematic for the P3DDT–CF/H–Si films, namely the large d-value (corresponding to the more relaxed or Form-I-like structure) toward the film–substrate interface, probably due to low viscosity (η_0), while the small d-value (corresponding to the more interpenetrating or Form-II-like structure) toward the top surface, probably due to high evaporation rate (E) of CF solvent. On the other hand, although the evaporation rate is low, the high viscosity of CB creates hindrance in the ordering and formation of the relaxed structure in the P3DDT–CB/Si films. The moderate values of both the parameters for the TL solvent help to enhance the ordering near the film–air interface overcoming the pinning effect in the

P3DDT–TL/H–Si films. The high evaporation rate of CF and high viscosity of CB probably create hindrance in the formation of continuous films on O–Si substrates at low speed, while moderate values of both the parameters for the TL solvent help to form continuous films on O–Si substrates even at low speed. The variation in the d-value in the low speed films is expected to be small, which is exactly observed for the latter types of films. Although the variation in the d-value in the P3DDT–TL/O–Si films is small, the relative fluctuation along the z-axis between adjacent lamellae is more compared to that in the P3DDT–CF/Si films. This can be inferred from the lower $\Delta\rho_m$-value, since adjacent stacks with lamellae slightly displaced from each other along the z-axis give rise to a diffused electron density of each layer, although their d-values do not differ much.

4 Conclusions

Structures of spin-coated P3DDT thin films, prepared using different polymer concentrations and solvents (*viz.* chloroform, toluene or chlorobenzene) were investigated using XR and UV-vis spectroscopy techniques. The strong dependence of the solvent and the substrate surface nature on the ordering or layering of the edge-on oriented P3DDT in the films, near the substrate and away from it, are observed from EDP. The ordering of P3DDT, if present near the film–substrate interface, is maximum there and decays exponentially along the film-thickness. The maximum value, the exponential decay length and the d-value and its deviation, however, vary with the solvent. For instance, the better ordered Form-I-like relaxed structure of higher d-value near the film–substrate interface and the less ordered interpenetrating Form-II-like structure of lower d-value toward the film–air interface are found in the films prepared from CF, which are related to the low viscosity and high evaporation rate, respectively, of the solvent. Similarly, less ordered mixed d-value structures are found throughout the films prepared from CB, which are related to the high viscosity of the solvent, even though its evaporation rate is low. In the film prepared from TL on the weakly hydrophobic H–Si substrate, no ordering is seen near the substrate due to less diffusion of P3DDT in TL and appreciable pinning on the substrate, while appreciable ordering near the film–air interface is seen, overcoming the pinning effect, due to the moderate values of both the viscosity and the evaporation rate of the solvent. In the film prepared from TL on the weakly hydrophilic O–Si substrate, ordering is found near the substrate due to less pinning on the substrate even though the diffusion of P3DDT in TL is less. The hindrance in the formation of the continuous film on the O–Si substrate at low speed from CF and CB is related to the high evaporation rate of CF and high viscosity of CB, while the continuous film from TL is related to the moderate values of both the parameters for TL. Such moderate values also help to form less variable d-values thus better ordering of P3DDT in the film prepared from TL on O–Si. However, the relative fluctuation between aggregates along the film-thickness is slightly more in the film prepared from TL compared to that prepared from CF.

Thus the ordering of edge-on oriented P3DDT due to π-stacked aggregates (responsible for charge delocalization) and the absence of any appreciable amount of coil-like P3DDT chains (responsible for charge localization) in spin-coated thin films, especially near the film–substrate interface, which has a strong influence on device properties, can be well regulated by varying the solvent, substrate surface nature and spinning speed.

Acknowledgements

References

1 *Organic Electronics: Materials, Processing, Devices and Applications*, ed. F. So, CRC, Boca Raton, FL, 2009.
2 A. Salleo, R. J. Kline, D. M. DeLongchamp and M. L. Chabinyc, *Adv. Mater.*, 2010, **22**, 3812–3838.
3 J. Rivnay, S. C. B. Mannsfeld, C. E. Miller, A. Salleo and M. F. Toney, *Chem. Rev.*, 2012, **112**, 5488–5519.
4 X. Guo, M. Baumgarten and K. Müllen, *Prog. Polym. Sci.*, 2013, **38**, 1832–1908.
5 F. Liu, Y. Gu, X. Shen, S. Ferdous, H.-W. Wang and T. P. Russell, *Prog. Polym. Sci.*, 2013, **38**, 1990–2052.
6 H. Sirringhaus, P. J. Brown, R. H. Friend, M. M. Nielsen, K. Bechgaard, B. M. W. Langeveld-Voss, A. J. H. Spiering, R. A. J. Janssen, E. W. Meijer, P. Herwig and D. M. de Leeuw, *Nature*, 1999, **401**, 685–688.
7 M. Brinkmann, *J. Polym. Sci., Part B: Polym. Phys.*, 2011, **49**, 1218–1233.
8 S. T. Shabi, E. Mikayelyan, S. Grigorian, U. Pietsch, N. Koenen, U. Scherf, N. Kayunkid and M. Brinkmann, *Macromolecules*, 2012, **45**, 5575–5585.
9 I. Roy and S. Hazra, *RSC Adv.*, 2015, **5**, 665–675.
10 R. J. Kline, M. D. McGehee, E. N. Kadnikova, J. Liu and J. M. J. Fréchet, *Adv. Mater.*, 2003, **15**, 1519–1522.
11 V. Causin, C. Marega, A. Marigo, L. Valentini and J. M. Kenny, *Macromolecules*, 2005, **38**, 409–415.
12 J.-F. Chang, B. Sun, D. W. Breiby, M. M. Nielsen, T. I. Sölling, M. Giles, I. McCulloch and H. Sirringhaus, *Chem. Mater.*, 2004, **16**, 4772–4776.
13 R. J. Kline, M. D. McGehee and M. F. Toney, *Nat. Mater.*, 2006, **5**, 222–228.
14 B. Meredig, A. Salleo and R. Gee, *ACS Nano*, 2009, **3**, 2881–2886.
15 W. D. Oosterbaan, J.-C. Bolsée, L. Wang, V. Vrindts, L. J. Lutsen, V. Lemaur, D. Beljonne, C. R. McNeill, L. Thomsen, J. V. Manca and D. J. M. Vanderzande, *Adv. Funct. Mater.*, 2014, **24**, 1994–2004.
16 M. Brinkmann and J.-C. Wittmann, *Adv. Mater.*, 2006, **18**, 860–863.
17 H. Yang, S. W. LeFevre, C. Y. Ryu and Z. Bao, *Appl. Phys. Lett.*, 2007, **90**, 172116.
18 D. Beljonne, J. Cornil, H. Sirringhaus, P. J. Brown, M. Shkunov, R. H. Friend and J.-L. Brédas, *Adv. Funct. Mater.*, 2001, **11**, 229–234.

19 X. M. Jiang, R. Österbacka, O. Korovyanko, C. P. An, B. Horovitz, R. A. J. Janssen and Z. V. Vardeny, *Adv. Funct. Mater.*, 2002, **12**, 587–597.

20 M. A. Ruderer, S. M. Prams, M. Rawolle, Q. Zhong, J. Perlich, S. V. Roth and P. Müller-Buschbaum, *J. Phys. Chem. B*, 2010, **114**, 15451–15458.

21 J. Ficker, A. Ullmann, W. Fix, H. Rost and W. Clemens, *J. Appl. Phys.*, 2003, **94**, 2638–2641.

22 J. Jaczewska, I. Raptis, A. Budkowski, D. Goustouridis, J. Raczkowska, M. Sanopoulou, E. Pamula, A. Bernasik and J. Rysz, *Synth. Met.*, 2007, **157**, 726–732.

23 K. Yoshino, Y. Manda, K. Sawada, M. Onoda and R. Sugimoto, *Solid State Commun.*, 1989, **69**, 143–146.

24 Y. Ohmori, M. Uchida, K. Muro and K. Yoshino, *Solid State Commun.*, 1991, **80**, 605–608.

25 S.-A. Chen and J.-M. Ni, *Macromolecules*, 1992, **25**, 6081–6089.

26 K. C. Park and K. Levon, *Macromolecules*, 1997, **30**, 3175–3183.

27 A. Babel and S. A. Jenekhe, *Synth. Met.*, 2005, **148**, 169–173.

28 I. F. Perepichka, D. F. Perepichka, H. Meng and F. Wudl, *Adv. Mater.*, 2005, **17**, 2281–2305.

29 W. Xu, L. Li, H. Tang, H. Li, X. Zhao and X. Yang, *J. Phys. Chem. B*, 2011, **115**, 6412–6420.

30 Y. Guo, Y. Jin and Z. Su, *Soft Matter*, 2012, **8**, 2907–2914.

31 I. K. Robinson and D. J. Tweet, *Rep. Prog. Phys.*, 1992, **55**, 599–651.

32 *X-Ray and Neutron Reflectivity: Principles and Applications*, ed. J. Daillant and A. Gibaud, Springer, Paris, 1999.

33 J. K. Bal and S. Hazra, *Phys. Rev. B: Condens. Matter Mater. Phys.*, 2009, **79**, 155405.

34 J. K. Bal, S. Kundu and S. Hazra, *Phys. Rev. B: Condens. Matter Mater. Phys.*, 2010, **81**, 045404.

35 P. Chatterjee and S. Hazra, *Soft Matter*, 2013, **9**, 9799–9806.

36 O. Werzer and R. Resel, *Macromolecules*, 2013, **46**, 3529–3533.

37 P. Chatterjee and S. Hazra, *J. Phys. Chem. C*, 2014, **118**, 11350–11356.

38 H. F. Okorn-Schmidt, *IBM J. Res. Dev.*, 1999, **43**, 351–366.

39 X. G. Zhang, *Electrochemistry of Silicon and its Oxide*, Kluwer Academic, New York, 2004.

40 J. K. Bal and S. Hazra, *Phys. Rev. B: Condens. Matter Mater. Phys.*, 2007, **75**, 205411.

41 J. K. Bal and S. Hazra, *Phys. Rev. B: Condens. Matter Mater. Phys.*, 2009, **79**, 155412.

42 P. Chatterjee, S. Hazra and H. Amenitsch, *Soft Matter*, 2012, **8**, 2956–2964.

43 S. Hazra, *Appl. Surf. Sci.*, 2006, **253**, 2154–2157.

44 L. G. Parratt, *Phys. Rev.*, 1954, **95**, 359–369.

45 P. J. Brown, D. S. Thomas, A. Köhler, J. S. Wilson, J.-S. Kim, C. M. Ramsdale, H. Sirringhaus and R. H. Friend, *Phys. Rev. B: Condens. Matter Mater. Phys.*, 2003, **67**, 064203.

46 J. Clark, C. Silva, R. H. Friend and F. C. Spano, *Phys. Rev. Lett.*, 2007, **98**, 206406.

47 F. C. Spano, *Acc. Chem. Res.*, 2010, **43**, 429–439.

48 L.-Y. Wong, R.-Q. Png, F. B. S. Silva, L.-L. Chua, D. V. M. Repaka, S.-Chen, X.-Y. Gao, L. Ke, S.-J. Chua, A. T. S. Wee and P. K. H. Ho, *Langmuir*, 2010, **26**, 15494–15507.

49 J. Catalán, *J. Phys. Chem. B*, 2009, **113**, 5951–5960.

50 G. M. Newbloom, S. M. Hoffmann, A. F. West, M. C. Gile, P. Sista, H.-K. C. Cheung, C. K. Luscombe, J. Pfaendtner and L. D. Pozzo, *Langmuir*, 2015, **31**, 458–468.

51 Material Safety Data Sheet, Fisher Scientific, http://www.fishersci.com.

52 Safety Data Sheet, LabChem, http://www.labchem.com.